# Subseasonal Variability of Surface Ocean Currents in the Bay of Bengal

**Midshipman 1/C Cody P. Spedero, Class of 2021;** *Advisor(s): Alexander R. Davies, Bradford S. Barrett, Joseph P. Smith*

## Background

During the summer months, the average surface wind over the Bay of Bengal (BoB) is out of the southwest. Conversely, the average surface wind during the winter months is out of the northeast (**Fig. 1**; *Kay et al. 2018*). As a result of the Indian Monsoon, average surface ocean currents in the BoB change dynamically (*Potemra et al., 1991*). During the summer monsoon, the average surface currents feature a counter-clockwise gyre with a strong southward East India Coastal Current (EEIC) (**Fig 2**; *Varkey et al. 1996*). About 100 km off the east coast of Sri Lanka, an intense northeastward current is surrounded by a loosely organized gyre and a broad eastward current south of 15°N. During the winter monsoon, the average EEIC is northward and associated with clockwise circulating gyres. There are westward average currents south of 10°N.

While the physical processes in the BoB are known to vary seasonally, less is known about how these processes are modulated on the subseasonal (30-60 day) time scale. The Madden-Julian Oscillation (MJO) is the leading mode of atmospheric variability at this scale and controls subseasonal patterns of circulation, pressure, and precipitation across the Tropics.

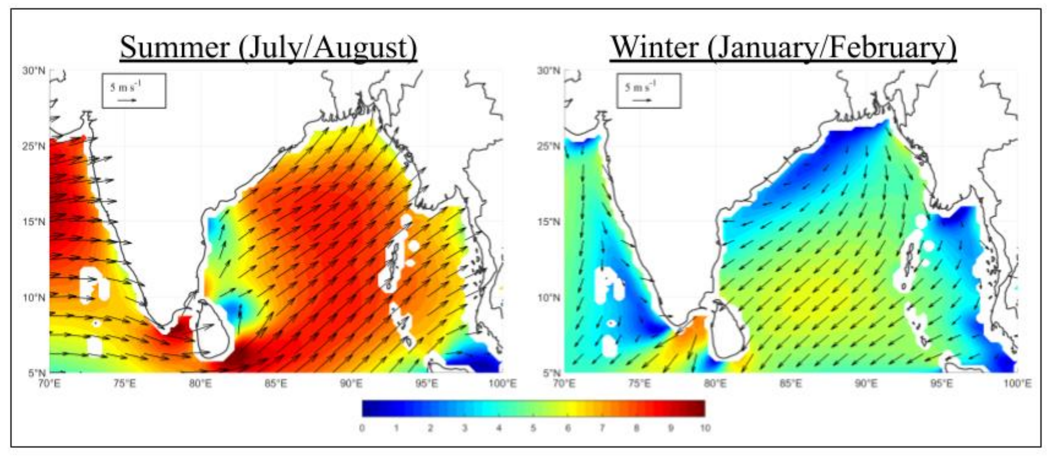


**Figure 1.** Mean 10-meter winds for winter (Jan and Feb) and summer (Jul and Aug) in the Bay of Bengal. The 10-meter winds show a seasonal reversal between the summer and winter months. Wind speeds are in $m\ s^{-1}$ (data source: ERA5 reanalysis).

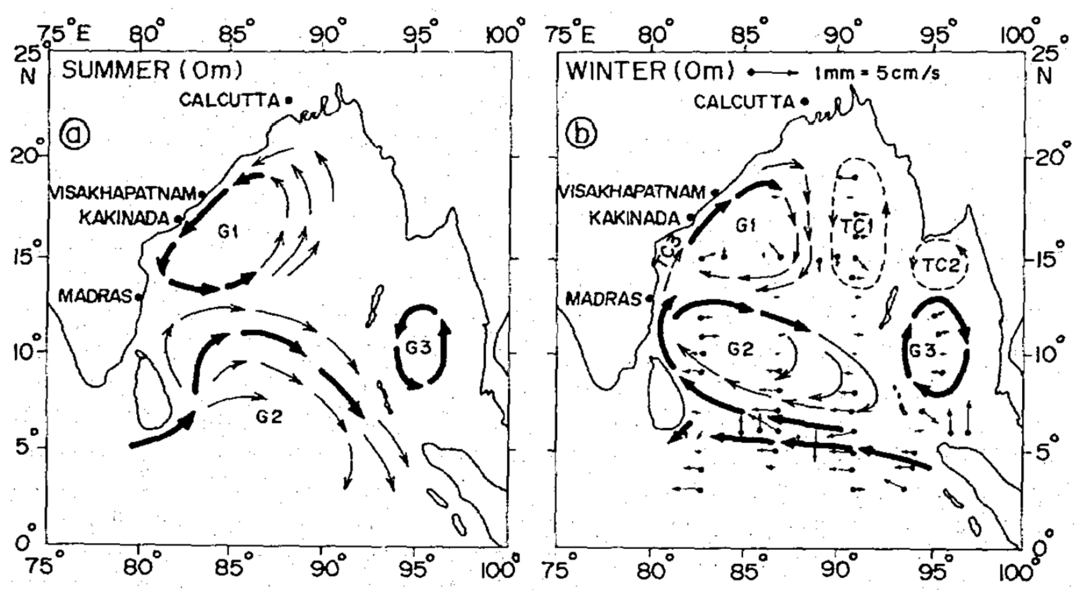


**Figure 2.** Schematic of the average surface ocean currents during the summer (left) and winter (right) monsoonal seasons in the Bay of Bengal (*Varkey et al. 1996* ).

***This study investigates the role of MJO in driving subseasonal surface wind and ocean current variability in the Bay of Bengal.***

## Data and Methods

### *Data sets analyzed*

Pentad standard anomalies of surface *u* and *v* surface current components from the Ocean Surface Current Analysis Real-time (OSCAR; *Bonjean and Lagerloef, 2002*) product and 10-m wind *U* and *V* wind components from the ERA5 global reanalysis (*Hersbach et al. 2020*) were calculated by subtracting the long-term (1993-2019) average and dividing by the standard deviation for each month pair (**Table 1**). The surface currents and 10-m wind standard anomalies were then binned by active phase of the Real-time Multivariate MJO (RMM; *Wheeler and Hendon 2004*) index with no time lag to capture direct effects. Statistical significance of the surface current and wind speed standard anomalies for each MJO phase and month pair was calculated using the two-sample *t*-test. Anomalies significant at the 95% confidence level were indicated.

### *Method to select MJO phases for analysis*

The hypothesis of this study is that surface ocean currents are modulated by the MJO via the MJO's influence on surface winds. To identify the month and phase pairs associated with the most significant anomalous surface wind forcing, the percentage of the *U* and *V* standard anomalies greater than 0.5 standard deviations over an area in the BoB defined by 77°E-94°E and 5°N-25°N were calculated for every MJO phase and month pair (**Table 1**). This spatial area was selected to focus the analysis between the Indian subcontinent and the Andaman Island chain. Four phases were found to have the greatest spatially coherent coverage of potentially impactful wind forcing: Phase 5 in May-June, Phases 4 and 6 in July-August, Phase 1 in September-October, and Phase 2 in November-December. Thus, the surface ocean current anomalies in those phases are investigated in this study.

| | Phase 1 | Phase 2 | Phase 3 | Phase 4 | Phase 5 | Phase 6 | Phase 7 | Phase 8 |
|---|---|---|---|---|---|---|---|---|
| Jan-Feb | u: 7.51%<br>v: 0% | u: 0%<br>v: 0% | u: 0%<br>v: 0% | u: 5.27%<br>v: 1.15% | u: 39.9%<br>v: 0% | u: 0%<br>v: 0% | u: 9.43%<br>v: 1.60% | u: 23.3%<br>v: 6.55% |
| Mar-Apr | u: 70.6%<br>v: 31.2% | u: 70.9%<br>v: 37.4% | u: 0%<br>v: 0% | u: 0%<br>v: 0% | u: 0%<br>v: 0% | u: 0%<br>v: 5.91% | u: 8.41%<br>v: 0% | u: 6.71%<br>v: 0% |
| May-Jun | u: 2.94%<br>v: 3.26% | u: 0.3%<br>v: 0.3% | u: 63.9%<br>v: 36.3% | u: 37.6%<br>v: 38.3% | **u: 13.9%**<br>**v: 56.8%** | u: 7.9%<br>v: 19% | u: 14.9%<br>v: 13.2% | u: 12%<br>v: 21% |
| Jul-Aug | u: 20.9%<br>v: 14.8% | u: 57.5%<br>v: 15.6% | u: 8.57%<br>v: 0.38% | **u: 65.2%**<br>**v: 13.7%** | u: 44.3%<br>v: 17.3% | **u: 70.6%**<br>**v: 23.5%** | u: 61.9%<br>v: 1.7% | u: 0.7%<br>v: 4.25% |
| Sep-Oct | **u: 78.1%**<br>**v: 72.5%** | u: 55.2%<br>v: 6.84% | u: 2.5%<br>v: 0% | u: 56.9%<br>v: 85.4% | u: 62.2%<br>v: 43% | u: 47.8%<br>v: 0% | u: 14.8%<br>v: 19% | u: 14.1%<br>v: 2.14% |
| Nov-Dec | u: 37.2%<br>v: 0.5% | **u: 63.6%**<br>**v: 4.5%** | u: 0%<br>v: 0% | u: 20%<br>v: 0% | u: 58.3%<br>v: ~0% | u: 50.5%<br>v: 0% | u: 13.9%<br>v: 29.4% | u: 0%<br>v: 0% |

**Table 1.** Percentage of 10-m surface wind anomalies greater than or equal to 0.5 standard deviations within the BoB area defined by 77°E-94°E, 5°N-25°N. Bolded values indicate the month/MJO phase pairs selected for further analysis.

***Acknowledgements.*** Special thanks to M. Alam for consultation on the month pair selection and analysis. This work was partially support by the U.S. Navy Office of Naval Research and the U.S. Naval Academy Office of Research and Scholarship.

## Results and Discussion

### *Analysis approach and conceptual framework*

Relatively uniform MJO modulation of the atmosphere tends to occur on the synoptic-to-planetary scales (*Hendon and Salby 1994*), which for the tropics is L ~ 500-5000 km (*Lau and Lau 1992*). However, in the ocean, the spatial scales tend to be an order of magnitude smaller than the atmosphere (*Lampitt et al. 2010*), and this mismatch in scales has the potential to complicate potential MJO modulation of the ocean. To identify strongest relationship between wind and ocean anomalies, field correlations were calculated for each month and phase pair for 77°E-94°E and 5°N-25°N. The results (not shown) do not suggest a basin-scale surface current response to even the most intense statistically significant wind forcing. Rather, the results suggest that only the most intense and spatially robust statistically significant atmospheric wind standard anomalies (**Table 1**) project onto the synoptic-scale surface ocean currents. The month pairs presented here represent modulation of the summer and winter/transitional monsoonal forcing by different MJO phases (**Fig. 3**) with a large sample size.

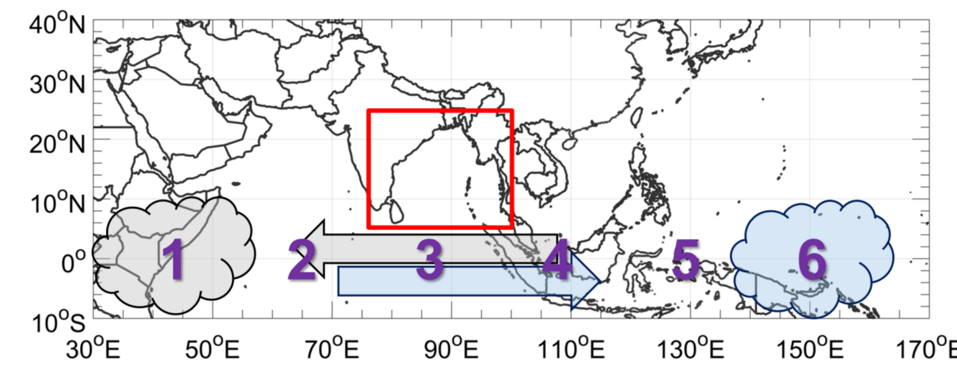


**Figure 3.** Schematic of winds during MJO phases. Red box is the study area and purple numbers are the approximate locations of the center of MJO convection, by phase. The gray cloud over phase 1 corresponds with the gray arrow indicating the expected wind anomaly during phase 1.The blue cloud over phase 6 corresponds with the blue arrow indicating the expected wind anomaly during phase 6. Figure augmented from *Donald et al., 2004*.

## July-August, Phase 6

The mean wind field across the BoB during July and August is from the southwest (**Fig. 4a**) and associated with the summer monsoon. The center of convection associated with MJO phase 6 is geographically located just east of the Maritime Continent (**Fig. 3**) and resulted in a statistically significant (stat. sig.) modulation of the positive *U* wind standard anomalies across the BoB (**Fig. 4b**). Stat. sig. *V* wind standard anomalies were weaker and limited to the eastern side of the BoB (**Fig. 4c**). The mean ocean currents in the BoB in July and August (**Figs. 2, 4**) feature a broader gyre to the north, southerly flow along the immediate Indian coast north of 15 °N, and easterly flow at 15 °N between 83 °E and 91 °E. In addition, there is an intense northeastward current off the coast of Sri Lanka that is likely resulting from the intense mean southwesterly wind forcing (**Fig. 4a**). **Figure 4e** shows broad and coherent stat. sig. positive *u* current standard anomalies along east of 90 °E and south of 10 °N that are co-located with strong positive *U* standard anomalies. In addition, there is a stat. sig. northward intensification of the current near the coast of Sri Lanka (**Fig. 4f**). Moreover, there is a stat. sig. intensification of the northern gyre in both the zonal and meridional directions, which is likely the result of the stat. sig. positive *u* current standard anomalies on the southern edge of the gyre.

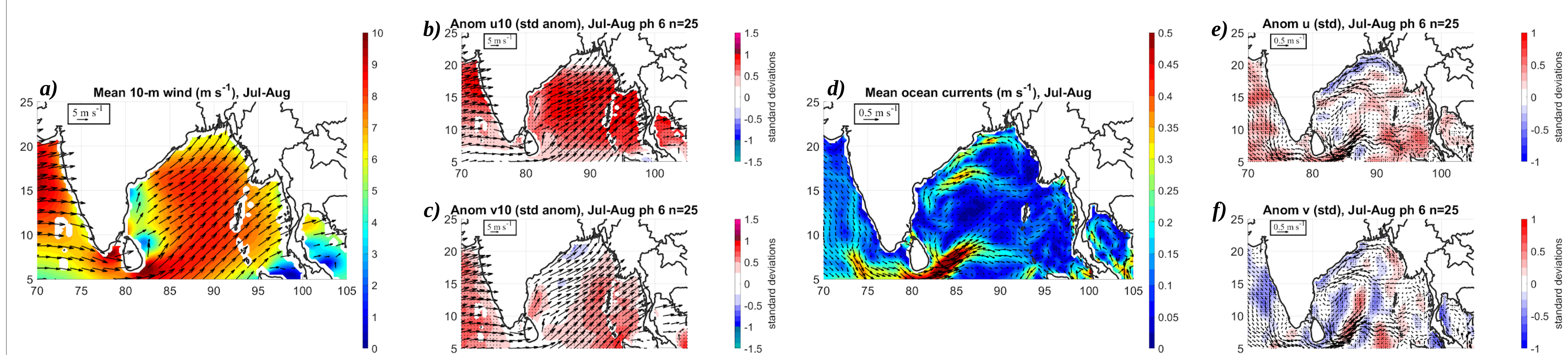


**Figure 4.** The magnitude (contoured) and quivered mean *a)* 10-m winds and *d)* surface ocean current in the BoB in July and August. *b)* The zonal 10-m wind (*U*) standard anomaly (contoured) with the Phase 6 average wind field (quivered). *c*) Same as *b)* but for the meridional 10-m wind (*V*) standard anomaly. *e)* The zonal 10-m surface ocean current (*u*) standard anomaly (contoured) with the Phase 6 average surface currents (quivered). *f)* Same as *e)* but for the meridional surface ocean current wind (*v*) standard anomaly. Statistically significant (95% level) standard anomalies are denoted with black dots in *b)*, *c)*, *e)*, and *f)*.

## September-October, Phase 1

September and October is a monsoonal transition season, where the intense southwesterly winds characteristic of the summer monsoon are diminished (**Fig. 5a**). The center of convection associated with MJO phase 1 is geographically located near the coast of Africa (**Fig. 3**), and in this phase, there are stat. sig. negative *U* wind standard anomalies across the entire BoB (**Fig. 5b**). Stat. sig. negative *V* wind standard anomalies were relatively weak and limited to central and eastern regions of the BoB (**Fig. 5c**). The mean ocean currents in the BoB during September and October (**Fig. 5d**) are also in transition with the remnant summer monsoon northern gyre (**Fig. 2,4d**) less organized. **Figure 5e** shows a broad and coherent area of stat. sig. negative *u* current anomalies south of 10 °N, resulting in a reversal of the overall current field (toward the west). The northeasterly mean current off the coast of Sri Lanka is weaker and shifted northward (**Fig. 5f**). The stat. sig. modulation of the current field (particular south of 10 °N) is more reminiscent of the mean currents during the winter monsoon (**Fig. 2**). This suggests that intense and coherent stat. sig. MJO variability may play a role in transitioning the currents in the BoB between the summer and winter monsoons.

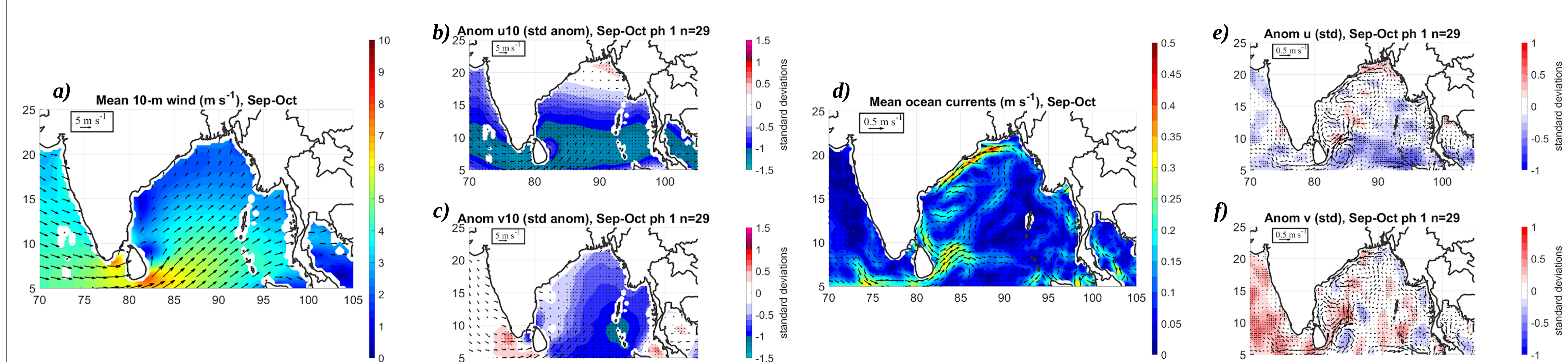


**Figure 5.** Same as **Figure** 4 but for September and October and MJO Phase 1.